

Materials & Design

Fatigue test data applicability for additive manufacture: A method for quantifying the uncertainty of AM fatigue data.

--Manuscript Draft--

Manuscript Number:	
Article Type:	Research Paper
Keywords:	Uncertainty quantification; additive manufacturing; powder bed fusion; certification; standards; error
Corresponding Author:	martin leary, PhD Melbourne, AUSTRALIA
First Author:	Jason Rogers, Undergraduate
Order of Authors:	Jason Rogers, Undergraduate Ma Qian, PhD Joe Elambasseril, PhD Colin Burvill, PhD Craig Brice, PhD Chris Wallbrink, PhD Milan Brandt, PhD martin leary, PhD
Abstract:	Additive manufactured (AM) components are increasingly being applied to fatigue-limited applications and are often safety-critical, necessitating confidence in the predicted fatigue response. The fatigue failure mode is highly sensitive to variations in loading, materials and geometry; therefore, published AM fatigue data must be accompanied by robust supporting documentation for confident adoption. International standards provide robust guidance on these documentation requirements; however, there are currently no formal methods for quantifying the uncertainty within published AM fatigue test data. A set of documentation criteria are proposed based on the core requirements of recognised standards for fatigue and AM test reporting. These documentation criteria form the basis for applicability indices that quantify the uncertainty of reported AM fatigue test data. The applicability indices offer a new way to evaluate the suitability of data for specific applications and are demonstrated for publicly available Powder Bed Fusion Ti-6Al-4V fatigue data. This large number of datasets are examined in terms of the influence of process variables on the observed fatigue response. These observations provide a reference for AM fatigue designers to be aware of the influence of relevant variables on fatigue response, as well as for AM fatigue researchers to identify strategic opportunities for novel contributions.
Suggested Reviewers:	Julian Booker J.D.Booker@bristol.ac.uk Johan Moverare johan.moverare@liu.se
Opposed Reviewers:	

Dear Editor:

Please find the manuscript entitled “*Fatigue test data applicability for additive manufacture: A method for quantifying the uncertainty of AM fatigue data applied to Ti-6Al-4V fabricated by PBF*” by Mr. Jason Rogers, Prof. Ma Qian, Dr. Joe Elambasseril, Prof. Colin Burvill, Prof. Craig Brice, Dr. Chris Wallbrink, Prof. Milan Brandt and Prof. Martin Leary. for possible publication in Materials and Design.

The current paper contributes to efforts regarding certification of powder bed fusion (PBF) Ti-6Al-4V for fatigue limited applications. In this research, a set of reporting criteria are proposed based on the core requirements of recognised standards for fatigue (ASTM E468-18) and AM test reporting (ASTM F2971-21). These reporting criteria allow vetting of existing data and guide best practice for future reporting of AM fatigue data. The updated reporting criteria are applied to a literature dataset to visualise the suitability of available data for safety-critical, fatigue limited design. As a complementary contribution, this large (N>30) literature fatigue dataset is examined in terms of the influence of independent design and process variables on the observed fatigue response. These observations provide a reference for AM fatigue designers to be aware of the influence of relevant variables on fatigue response, as well as for AM fatigue researchers to identify strategic opportunities for novel contributions.

We believe this article deserves attention not only in the field of certification and design, but also for PBF Ti-6Al-4V fatigue response and will attract considerable interest from your readership.

Sincerely Yours,

Jason Rogers

PhD candidate, RMIT University

Centre for Additive Manufacturing, School of Engineering,

Royal Melbourne Institute of Technology, Melbourne, Victoria, Australia

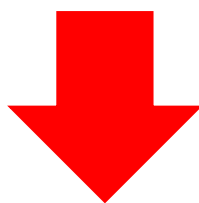


+ 61 428 955 563

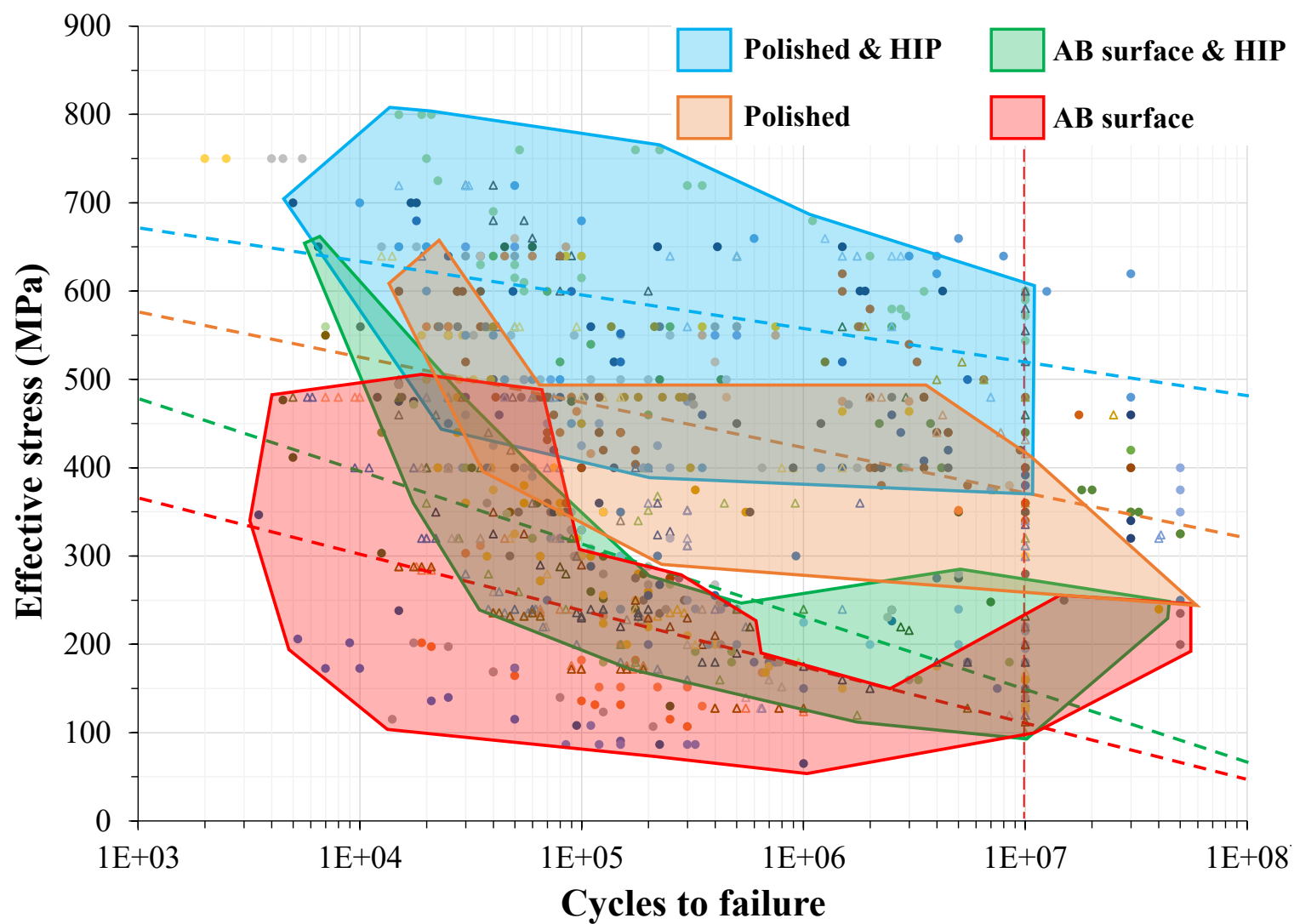
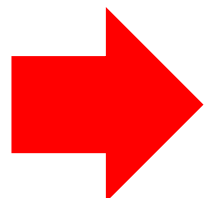


martin.leary@rmit.edu.au

**AM reporting standard:
ASTM F2971**



**AM-relevant
fatigue
documentation
criteria**



Highlights

- We propose reporting criteria to allow vetting of existing data and best practice for future reporting of AM fatigue data.
- On average 72% of relevant fatigue test information is reported for PBF Ti-6Al-4V.
- Omitted fatigue test information includes tensile properties and microstructure characterisation.
- An extensive fatigue data set allows clear comparison on the effects of post processing for PBF Ti-6Al-4V.

RMIT Classification: Trusted

Fatigue test data applicability for additive manufacture: A method for quantifying the uncertainty of AM fatigue data.

Jason Rogers¹, Ma Qian¹, Joe Elambasseril¹, Colin Burvill², Craig Brice³,
Chris Wallbrink⁴, Milan Brandt¹, Martin Leary¹

1: RMIT Centre for Additive Manufacture, RMIT University,
Melbourne Australia, martin.Leary@rmit.edu.au

2: University of Melbourne, Department of Mechanical Engineering,
colb@unimelb.edu.edu

3: Additive Manufacturing Program, Colorado School of Mines,
craigabrice@mines.edu

4: Defence Science & Technology, christopher.wallbrink@defence.gov.au

Abstract

Additive manufactured (AM) components are increasingly being applied to fatigue-limited applications and are often safety-critical, necessitating confidence in the predicted fatigue response. The fatigue failure mode is highly sensitive to variations in loading, materials and geometry; therefore, published AM fatigue data must be accompanied by robust supporting documentation for confident adoption. International standards provide robust guidance on these documentation requirements; however, there are currently no formal methods for quantifying the uncertainty within published AM fatigue test data. A set of documentation criteria are proposed based on the core requirements of recognised standards for fatigue and AM test reporting. These documentation criteria form the basis for *applicability indices* that quantify the uncertainty of reported AM fatigue test data. The *applicability indices* offer a new way to evaluate the suitability of data for specific applications and are demonstrated for publicly available Powder Bed Fusion Ti-6Al-4V fatigue data. This large number of datasets are examined in terms of the influence of process variables on the observed fatigue response. These observations provide a reference for AM fatigue designers to be aware of the influence of relevant variables on fatigue response, as well as for AM fatigue researchers to identify strategic opportunities for novel contributions.

Keywords: *Uncertainty quantification, additive manufacturing, powder bed fusion, certification, standards, error.*

Table 1: Table of abbreviations

Abbreviations	Definitions
3PB	Three-point bending
4PB	Four-point bending
AB	As-built
AM	Additive manufacturing
BD	Build direction
EB-PBF	Electron based powder bed fusion
HIP	Hot isostatic pressing
HT	Heat treated
LB-PBF	Laser based powder bed fusion
MCD	Machined
PBF	Powder bed fusion
R_a	Arithmetic mean roughness
RBB	Rotating beam bending
R_v	Maximum surface profile valley depth
R_z	Maximum surface profile height within a sample length
TB	Tribofinished
UTS	Ultimate tensile strength
YS	Yield strength

1 Introduction

Published fatigue data is critical for the design of fatigue-limited systems as it alleviates the need for costly and time-consuming custom fatigue tests. This published data is particularly relevant to characterise emerging materials and manufacturing technologies such as Additive Manufacturing (AM). However, when fatigue data is insufficiently documented, its utility for design may be restricted due to uncertainties in fatigue response.

The fatigue response of a material is substantially influenced by loading and environment; material and microstructure; component geometry and geometric defects [1]. The contribution of these factors can be summarised as follows:

- Loading and environment:** Changing fatigue loading conditions results in changes in fatigue response for otherwise similar material and manufacturing conditions. For example, low cycle fatigue response, exhibiting nominally plastic deformation, is dominated by crack growth whereas bulk material properties largely dominate the observed fatigue strength. High cycle fatigue, exhibiting nominally elastic deformation, is dominated by crack initiation where surface defects and flaws are more influential [2]. For sinusoidal loading, the fatigue response is sensitive to the load ratio (R =minimum load/maximum load). Where, fully reversed loading, $R=-1$, is more severe than fully tensile loading, $R=0.1$. Methods exist that attempt to accommodate the effects of load ratio on fatigue response [3] (Section 4.1). However, in general it is necessary that the fatigue response of data collected using different load ratios are not compared directly. Fatigue response is sensitive to the loading environment; For example, the fatigue life of aluminium at ultrasonic frequencies is heavily influenced by humid environments [4]; and titanium is susceptible to heat ablation under fatigue loading at high test frequencies [5].
- Material and microstructure influence fatigue response.** This influence is significant in Powder Bed Fusion (PBF) which exhibits rapid solidification (and therefore distinct microstructures) when compared to other manufacturing methods such as casting. For example in Ti-6Al-4V alloy, the large thermal gradients associated with laser-based (LB) PBF have been observed to result in fine, acicular α' microstructure and columnar prior β grain boundaries, parallel to the build direction [6]. Electron-beam (EB) PBF has a higher bed temperature, resulting in smaller thermal gradients during manufacture, potentially resulting in a near equilibrium alpha-beta microstructure for Ti-6Al-4V [7]. Although both EB-PBF and LB-PBF Ti-6Al-4V display material anisotropy with prior β grains aligned with the build direction [8], orientation of α and α' is stochastic with an orientation relationship to β grains [9]. The fine martensite typical of LB-PBF Ti-6Al-4V enhances material strength, while the coarser α - β microstructure typical of EB-PBF Ti-6Al-4V enhances material ductility [10]. The large thermal gradients occurring during LB-PBF induce residual stresses in components [6], of which tensile residual stresses are detrimental to fatigue performance [11]. However, due to higher relative processing temperatures in EB-PBF, residual stresses are reduced [12]. Heat treatment is commonly used to relieve

residual stress in components [13], this will also result in a coarser microstructure [14]. Hot isostatic pressing (HIP) improves fatigue response by closing internal pores due to the combination of high temperature and isostatic pressure [15]. Furthermore, HIP is shown to refine local microstructures surrounding internal defects [16]. Despite the opportunities associated with HIP, it has been observed that closed pores can re-open on further high temperature heat treatments such as β annealing [64].

- **Component geometry and surface defects** may induce stress concentrations and in turn reduce component fatigue life [17]. In the case of AM, there are a large number of manufacturing variables that can affect component geometry. Surface roughness has been shown to be the most detrimental factor in the fatigue life of PBF Ti-6Al-4V and has been studied extensively [18-20]. For example, layer height impacts surface roughness and internal defect formation, in turn affecting fatigue life [21]. The manufacturing angle of components affects the surface roughness through stair stepping, dross formation and adhered powder particles [22].

If these influential factors are undisclosed, uncertainty exists in fatigue life prediction that limits the applicability of this reported data for safety-critical design. Methods have been proposed to characterise and assess the applicability of fatigue test data and have found that published fatigue data may “exhibit incomplete documentation” [23]. These methods are defined for traditional materials and manufacturing methods and do not account for the fatigue-relevant aspects of AM. A method for comparing the quality of reported AM fatigue data is urgently required to characterise the uncertainty of published data for safety-critical design and certification.

Formal standards exist to ensure that published test data is accompanied by the supporting information necessary for confident test replication. *ASTM E468-18* defines ‘Standard Practice for Presentation of Constant Amplitude Fatigue Test Results for Metallic Materials’ [24], and thereby provides an authoritative reference for the minimum requirements for the reporting of fatigue data. Similarly, *ASTM F2971-21* ‘Standard Practice for Reporting Data for Test Specimens Prepared by Additive Manufacturing’ [25] systematically defines what data should be reported when AM materials are used for mechanical testing. *ASTM E468-18* is based on materials produced using traditional methods, therefore considerations of build orientation, powder size distribution, powder recycling and other aspects relevant to AM are not considered. Similarly, the AM reporting standard *ASTM F2971-21* is not concerned with the specific requirements of fatigue test procedures.

This research proposes a method for the characterisation of applicability of reported fatigue-test data for AM. The method considers the specific process, design, and material aspects of AM. It can be applied to determine the relevance of reported data for specific scenario and to provide guidance to AM fatigue researchers on what documentation is required for effective reporting. The proposed method is demonstrated using publicly available PBF Ti-6Al-4V fatigue data. This research provides insights on the general quality of reported data, examines a large number ($N>30$) of datasets to understand how

the influence of design and process variables affect fatigue response, and identifies opportunities for future research.

2 Documentation criteria and applicability indices

The uncertainty inherent in published fatigue data can be objectively assessed with reference to formal standards. For example, previous research has quantified the uncertainty of published fatigue data with reference to international fatigue test reporting standards, but does not accommodate the specific attributes of AM specimens that are relevant to the fatigue failure mode [23]. To extend the applicability of previous research, a formal method for quantifying the uncertainty of reported AM fatigue test data was developed with reference to existing standards for the reporting of metallic fatigue test data (*ASTM E468-18*) and additively manufactured test specimens (*ASTM F2971-21*).

Documentation criteria were selected from these standards as the essential reporting criteria of the standard; optional items were excluded from this analysis. Documentation criteria were categorised as: fatigue relevant (ω_{F_i} , Section 3.1, Table 2); AM relevant (ω_{AM_i} , Section 3.2, Table 3); and combined AM-fatigue relevant (ω_{C_i} , Section 3.3, Table 4). According to the selected documentation criteria (Section 2), documentation criteria are scored as fully (1.0), partially (0.5) or failing (0) to satisfy the intention of the associated standards.

Applicability indices, α , quantify the applicability of each dataset as the average value of the associated documentation criteria (Eq. 1-3). Applicability indices provide a robust method for AM fatigue designers to evaluate the applicability of a proposed fatigue data set for design purposes. For AM fatigue researchers, the applicability indices provide an opportunity to identify additional complimentary experiments that enhance the applicability of available fatigue data.

$$\alpha_F = \frac{1}{n} \sum_{i=0}^n \omega_{F_i} \quad (1)$$

$$\alpha_{AM} = \frac{1}{n} \sum_{i=0}^n \omega_{AM_i} \quad (2)$$

$$\alpha_C = \frac{1}{n} \sum_{i=0}^n \omega_{C_i} \quad (3)$$

Applicability indices are defined for: fatigue relevant documentation criteria (Table 2), AM relevant documentation criteria (Table 3), and *combined* AM-fatigue criteria (Table 5).

2.1 Fatigue relevant documentation criteria

The initiation and propagation of a fatigue crack is influenced by microstructural defects and slip planes, operational environment, material toughness, and stress intensity profiles. Raw material properties and the state of the material after any post processing steps should be documented to understand the correlation with observed experimental results. The documentation criteria of Table 2 are selected as being of critical importance to the reporting of fatigue test data for metallic materials as specified by *ASTM E468-18* [24].

Table 2: Fatigue Documentation Criteria (ω_F) selected according to *ASTM E468-18* for fatigue reporting of metallic materials.

ASTM reference	Documentation Criteria (ω_F)	Fatigue relevant documentation criteria
<i>E468 – 5.1.1</i>	$\omega_F\ 1$	Material specification i.e. Ti-6Al-4V.
	$\omega_F\ 2$	Chemical composition.
	$\omega_F\ 3$	Raw material surface condition.
<i>E468 – 5.1.2.1</i>	$\omega_F\ 4$	Tensile strength or yield strength at a specified onset.
	$\omega_F\ 5$	Elongation in a specified gage length.
	$\omega_F\ 6$	Reduction of area when applicable.
	$\omega_F\ 7$	Designation of the test (i.e. E8/E8M).
<i>E468 – 5.2.1</i>	$\omega_F\ 8$	Drawing showing dimensions of fatigue specimen.
	$\omega_F\ 9$	Geometry, <i>Kt</i> of notch, notched tensile strength.
<i>E468 – 5.3.1</i>	$\omega_F\ 10$	Type of process used to form specimen.
	$\omega_F\ 11$	Heat treatment.
	$\omega_F\ 12$	Surface treatment.
	$\omega_F\ 13$	Polishing sequence and direction.
<i>E468 – 6.1</i>	$\omega_F\ 14$	Statistical techniques used to design test program.
<i>E468 – 6.2.1</i>	$\omega_F\ 15$	Type of test machine.
	$\omega_F\ 16$	Functional characteristic test (i.e. pneumatic).
	$\omega_F\ 17$	Frequency of force application.
	$\omega_F\ 18$	Forcing function i.e. sinusoidal, square wave etc.
	$\omega_F\ 19$	Force monitoring and force verification procedure.
	$\omega_F\ 20$	Number of testing machines used
<i>E468 – 6.3.1</i>	$\omega_F\ 21$	Type of fatigue test
	$\omega_F\ 22$	Derivation of dynamic stress on test section.
	$\omega_F\ 23$	Failure criterion.
	$\omega_F\ 24$	Number of cycles to runout.
<i>E468 – 6.4</i>	$\omega_F\ 25$	Average value and range of temperature and humidity.
<i>E468 – 6.5</i>	$\omega_F\ 26$	Reason for test termination for each specimen.
	$\omega_F\ 27$	Description of fracture surface and failure origin.
<i>E468 – 7.2.1</i>	$\omega_F\ 28$	Graphical presentation in the form of S-N curve...Including material, tensile strength, surface condition, <i>Kt</i> of notch, type of fatigue test, stress ratio, frequency, test environment temperature.

2.2 AM relevant documentation criteria

The intricacies of additive manufacturing mean that there are a large number of variables which can impact the mechanical properties of test specimens, including: build orientation and position within the build volume; layer thickness and power settings; powder morphology and powder recycling procedures [1]. Build orientations with surfaces inclined close to the horizontal plane promote high surface roughness, which is detrimental to fatigue performance, especially on downward facing surfaces. Non-optimal manufacturing parameters will also increase surface roughness and promote damaging internal defects. According to *ASTM F2971-21* (Standard Practice for Reporting Data for Test Specimens Prepared by Additive Manufacturing) the criteria listed in Table 3 are of critical importance when reporting information related to the mechanical response of AM components [25].

Table 3: AM Documentation Criteria (ω_{AM}) selected from *ASTM F2971-21* standard practice for reporting data for test specimens prepared by Additive Manufacturing.

<i>ASTM</i> reference	Documentation Criteria (ω_{AM})	AM relevant documentation criteria
<i>F2971 – 5.1.1.1</i>	ω_{AM_1}	Description and preparation of AM feedstock.
	ω_{AM_2}	Procedure for re-using feedstock material.
<i>F2971 – 5.1.1.4</i>	ω_{AM_3}	A description of all non-standard production processes used.
<i>F2971 – 5.1.1.3</i>	ω_{AM_4}	All standard processes used to produce the specimen from feedstock.
	ω_{AM_5}	Placement and orientation of specimen in build chamber.
<i>F2971 – 5.1.2.1</i>	ω_{AM_6}	Toleranced dimensions of test specimens.
	ω_{AM_7}	Test plan.
	ω_{AM_8}	Test procedures.
	ω_{AM_9}	Non-destructive inspection procedures and results.
<i>F2971 – 5.1.2.2</i>	ω_{AM_10}	A description of all non-standard test methods used.
<i>F2971 – 5.1.2.3</i>	ω_{AM_11}	Post processing steps not highlighted by previous criteria.

2.3 Combined documentation criteria relevant to the fatigue of AM

A correlation matrix is presented to compare the documentation criteria selected for fatigue (*ASTM E468-18*) and AM (*ASTM F2971*) reporting standards (

Table 4). The following observations are relevant:

- This matrix shows approximately 20% correlation between the documentation criteria selected from fatigue and AM reporting standards.
- Of these identified criteria, there are approximately double the number of high correlations ($N = 42$) than moderate ($N = 20$) correlations.
- 100% of the AM documentation criteria correlate with at least one fatigue relevant documentation criterion. It should be noted that some of these are moderate correlations only. Conversely, only 86% of fatigue relevant documentation criteria correlate with at least one AM documentation criterion.
- Powder recycling, ω_{AM_2} , build orientation, ω_{AM_5} and non-destructive inspection procedures, ω_{AM_9} , only have moderate correlation with a fatigue relevant documentation criterion. The implication being that these AM attributes are not well accounted for in the fatigue standard.
- Tensile properties, ω_{F_4} , elongation, ω_{F_5} , reduction of area, ω_{F_6} , fatigue S-N response, ω_{F_28} , have no correlation with the identified AM documentation criteria. The implication being that these fatigue attributes are not accounted for in the AM standard.
- Reporting of standard, ω_{AM_8} , and non-standard, ω_{AM_10} , test procedures correlated with fourteen and twelve of the fatigue relevant documentation criteria respectively. This outcome is due to the broad nature of these documentation criteria as they correlate with multiple, highly specific, documentation criteria from the fatigue reporting standards.
- The reporting of standard production procedures, ω_{AM_3} , non-standard production procedures, ω_{AM_4} , and test plans, ω_{AM_7} , are in correlation with nine, nine and eight of the identified fatigue documentation criteria, respectively. Again, this outcome is due to the broad nature of the associated AM criteria.
- Material specification, ω_{F_1} , has the highest correlation with the identified AM relevant documentation criteria. Understanding material properties is a fundamental aspect of design, manufacturing and testing, thus resulting in the broad correlation.

Table 4: Correlation matrix between fatigue, ω_F , and AM relevant documentation criteria, ω_{AM} . Documentation criteria with *high* (solid circle) and moderate (open circle) correlation identified. AM documentation criteria with a large number of correlations identified in red border boxes.

		AM Relevant Documentation Criteria										
		ω_{AM_1}	ω_{AM_2}	ω_{AM_3}	ω_{AM_4}	ω_{AM_5}	ω_{AM_6}	ω_{AM_7}	ω_{AM_8}	ω_{AM_9}	ω_{AM_10}	ω_{AM_11}
Fatigue Relevant Documentation Criteria	ω_{F_1}	●	○	○	○			○				
	ω_{F_2}	●		○	○							
	ω_{F_3}	●		○	○							
	ω_{F_4}											
	ω_{F_5}											
	ω_{F_6}											
	ω_{F_7}								●		●	
	ω_{F_8}			○	○	○	●					
	ω_{F_9}			○	○		●	○				
	ω_{F_10}		○	●	●			○				
	ω_{F_11}			●	●			●				●
	ω_{F_12}			●	●			●				●
	ω_{F_13}			●	●			●				●
	ω_{F_14}							●	●		●	
	ω_{F_15}								●		●	
	ω_{F_16}								●		●	
	ω_{F_17}								●		●	
	ω_{F_18}								●		●	
	ω_{F_19}								○		○	
	ω_{F_20}								○			
	ω_{F_21}							●	●		●	
	ω_{F_22}								●		●	
	ω_{F_23}								●		●	
	ω_{F_24}								●		●	
	ω_{F_25}								○		○	
	ω_{F_26}								●		●	
	ω_{F_27}									○		
	ω_{F_28}											

In order to minimise uncertainty and ensure standard documentation procedures for AM fatigue data, combined documentation criteria (ω_C , Table 5), are selected to represent both fatigue (*E468-18*) and AM (*F2971-21*) reporting standards according to the following basis:

Basis 1: ASTM E468-18 documentation criteria were chosen when required to accompany an S-N curve and as such are assumed to be critically important¹.

Basis 2: ASTM F2971-21 documentation criteria were chosen because they were not effectively correlated with *ASTM E468-18* according to the comparison matrix (Table 4).

¹ This logic was applied for the investigation of fatigue data reporting for traditional manufacturing [23].

Table 5: Combined Documentation Criteria (ω_C) selected according to Basis 1 (*) or Basis 2 (^). Relevant sub-sections of original standards are shown for reference.

ASTM reference	Combined documentation criteria	Original documentation criteria
E468 – 5.1.1	ω_{C_1} *	Material specification e.g. Ti-6Al-4V.
E468 – 5.1.1	ω_{C_2} ^	Chemical composition of feedstock.
E468 – 5.1.1	ω_{C_3} *	Surface condition.
E468 – 5.1.2.1	ω_{C_4} *	Tensile strength.
E468 – 5.1.2.2	ω_{C_5} ^	Microstructure grain size and phase composition.
E468 – 5.3.1	ω_{C_6} *	Heat treatment.
E468 – 5.3.1	ω_{C_7} ^	Type of process used to form the specimen.
E468 – 6.2	ω_{C_8} *	Type of fatigue test.
E468 – 6.2.1	ω_{C_9} *	Frequency of force application.
E468 – 6.3	ω_{C_10} *	Temperature during testing.
E468 – 7.2.1	ω_{C_11} *	Graphical presentation of fatigue results.
E468 – 7.2.1.1	ω_{C_12} *	Stress ratio.
F2971 – 5.1.1.1	ω_{C_13} ^	Powder size distribution.
F2971 – 5.1.1.1	ω_{C_14} ^	Process for re-using feedstock/powder.
F2971 – 5.1.1.3	ω_{C_15} ^	Placement and orientation in chamber.
F2971 – 5.1.2.1	ω_{C_16} ^	Number of samples used for fatigue testing.
F2971 – 5.1.2.1	ω_{C_17} ^	Dimensions of test specimens w/tolerances.

3 Applicability of reported Ti-6Al-4V PBF data

The methods proposed in this paper aim to quantify the uncertainty of reported fatigue test data in additive manufacturing (AM) studies. These methods have been utilized in the analysis of recent² fatigue test data for Ti-6Al-4V specimens fabricated through Laser-Based (LB) or Electron Beam (EB) Powder Bed Fusion (PBF) processes. These reported data are then analysed and ranked according to the Fatigue (ω_F), AM (ω_{AM}) and Combined Documentation Criteria (ω_C) [24, 25], with the following observations (Figure 1 and Figure 2):

- The nominal material specification (ω_{C_1}) and manufacturing method (ω_{C_7}) are reported by all the fatigue data sources examined. All other documentation criteria are omitted by at least some of the examined sources.
- The mean applicability index for the combined documentation criteria, $\bar{\alpha}_C$, was 72%.
- The mean applicability indices for the fatigue and AM relevant criteria are 64% and 67%, respectively. The slight bias toward higher documentation criteria for the combined metric suggests that the authors of the assessed PBF fatigue data are naturally focussed on data that is relevant to both AM and fatigue reporting. The relatively low values of the reported averages, indicates an opportunity for increased documentation in the general literature.

² within the last 10 years.

- Of the assessed documentation criteria, powder recycling procedures ($\omega_{c_{14}}$), was most commonly omitted from fatigue test documentation, despite the known impact on powder size distribution, particle size distribution and the formation of lack of fusion defects and flowability [26].
- The average temperature range during fatigue testing ($\omega_{c_{10}}$), material strength (ω_{c_4}), microstructure description (ω_{c_5}) and chemical composition (ω_{c_2}) were omitted by at least 40% of the analysed papers.
- Post processing applied to samples was well reported with surface condition (ω_{c_3}) and heat treatment (if any) (ω_{c_6}) both reported by 97% of analysed papers.
- None of the studied references achieve 100% applicability for any of the identified applicability indices (Figure 2).

The observations of PBF Ti-6Al-4V fatigue test data reveal that reported data is commonly incomplete in terms of the documentation requested by the associated standards. These omissions are asymmetrically distributed, for example material type and processing method are always reported. However, the associated microstructure, chemical composition and powder recycling protocols are typically omitted (Figure 1). The examination of inadequate documentation aligns with previous research reporting fatigue test data from traditionally manufactured specimens [23], and reaffirms the need for caution when designing for fatigue to prevent uncertainties caused by ambiguous documentation of fatigue test data, particularly for complex manufacturing methods such as PBF.

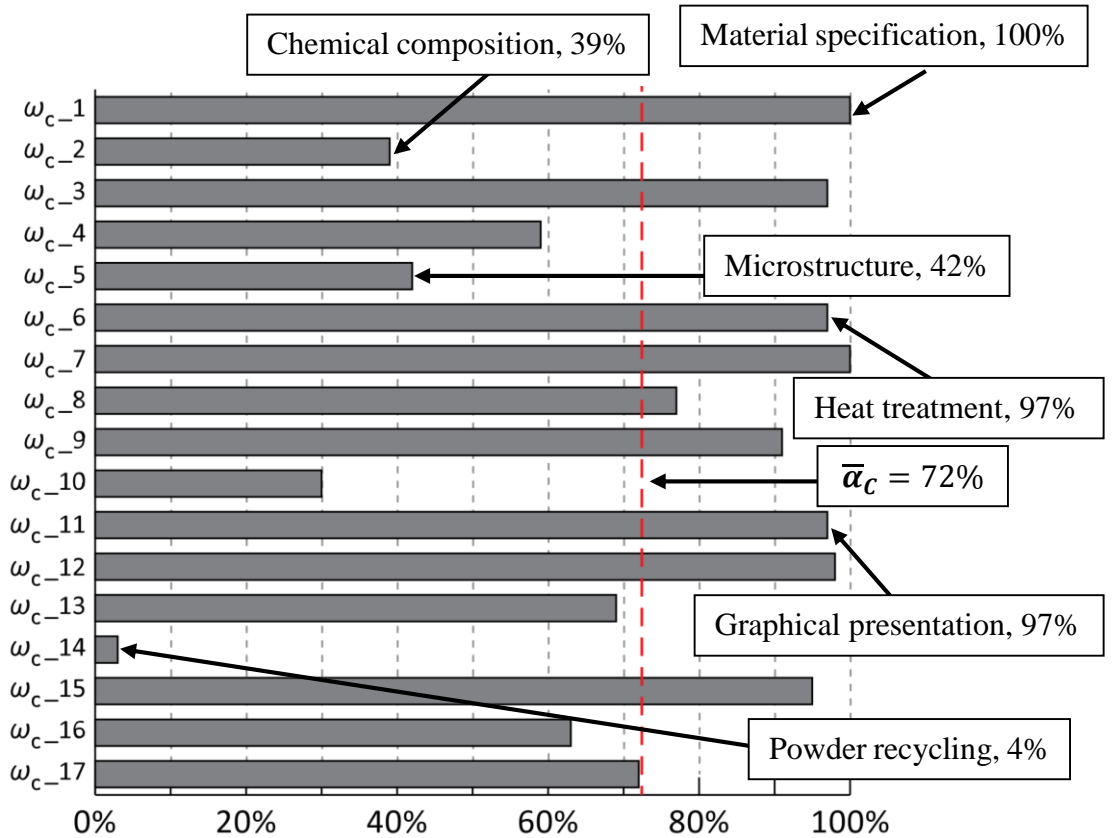


Figure 1: The percentage satisfaction of each of the combined documentation criteria, ω_c , listed in Table 5, based on 32 AM fatigue resources [5, 12, 26-55].

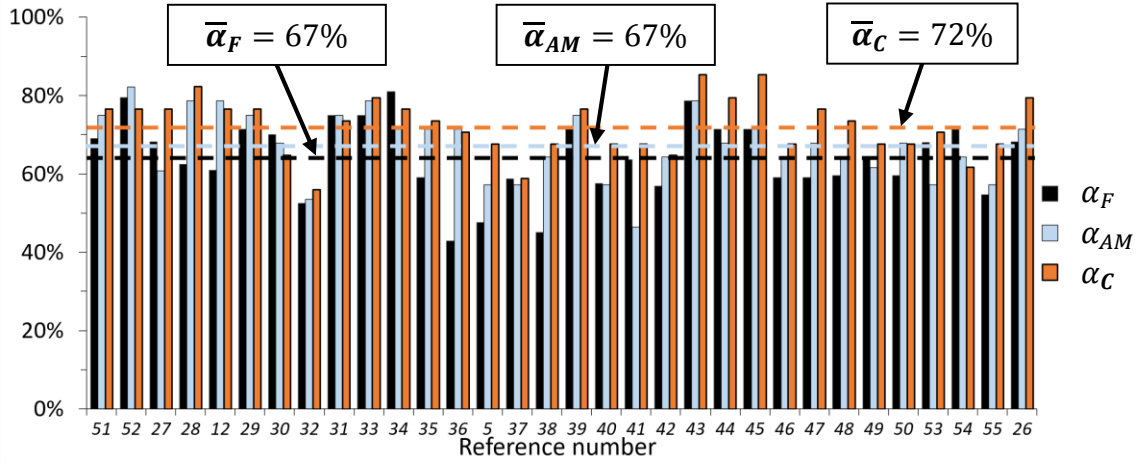


Figure 2: Applicability indices for fatigue, AM and combined documentation criteria, α_F , α_{AM} and α_C , for all published resources included in this analysis. The average applicability indices are indicated.

4 General observations of AM fatigue test data

The set of PBF Ti-6Al-4V fatigue test data ($N > 30$) provides a substantial opportunity to gain insight into the effect of design and process variables on observed fatigue response. These observations provide insight into the effect of these independent variables as well as to confirm the importance of their appropriate documentation for fatigue test reporting. Observed fatigue response is briefly analysed in terms of the: tensile and fatigue properties (Section 4.1); surface roughness (Section 4.2) and microstructure and chemistry (Section 4.3).

4.1 Fatigue and tensile property analysis

The experimental fatigue data from all 32 papers [5, 12, 26-55] that were manufactured using LP-PBF or EB-PBF have been summarised in the following sections. This includes the S-N curves (Figure 3), fatigue test conditions (Table 6), mechanical and roughness properties of specimens with as-built (Table 7) and processed surfaces (Table 8), as well as those with HIP applied (Table 9). To enable comparison between datasets, data obtained from notched specimens, ultrasonic, and strain-controlled testing was excluded, and the fatigue data was normalised to the effective stress, σ_{eff} , for $R = -1$ using Walker's method (equation 4). The following observations are made:

- The pronounced variability between observed fatigue response in Figure 3 in terms of the effective stress associated with a given fatigue life is influenced by post processing. Samples with as-built (AB) surfaces or polished surfaces, as well as those subjected to Hot Isostatic Pressing (HIP) are highlighted to illustrate the influence of these post processing variables on fatigue response.
- As-built surfaces are associated with the lowest observed effective stress values, with minima occurring below 100MPa.
- Polished surfaces, conversely, show a substantially higher effective stress by comparison to the as-built surfaces. This outcome is related to the substantial

influence of as-built surface roughness on stress concentrations and the crack initiation phase of the fatigue failure mode (this outcome is discussed in detail in Section 4.2).

- The HIP process also has a substantial impact on the observed fatigue response, with both as-built and polished surfaces showing a significant improvement in observed fatigue strength following the HIP process (the metallurgical aspects of this observation are discussed in detail in Section 4.3).
- It should be noted that the observed benefit of HIP on as-built surfaces, based on the assessed data, appears to occur below 1E7 cycles. Additionally, for 1E7 cycles, the general response of as-built surfaces with and without HIP is similar.
- When analysing fatigue test conditions in Table 6, the most common stress ratio, R , is 0.1 and the most common test method is uniaxial.
- For the fatigue data assessed, monotonic tensile properties are typically not reported. Specifically, for specimens with as-built surface conditions (as presented in Table 7), processed surface conditions (as presented in Table 8), and HIP (as presented in Table 9), only 59%, 20%, and 15% of the fatigue data included tensile properties, respectively.

$$\sigma_{eff} = \sigma_{max} \left(\frac{1 - R}{2} \right)^{0.28} \quad (4)$$

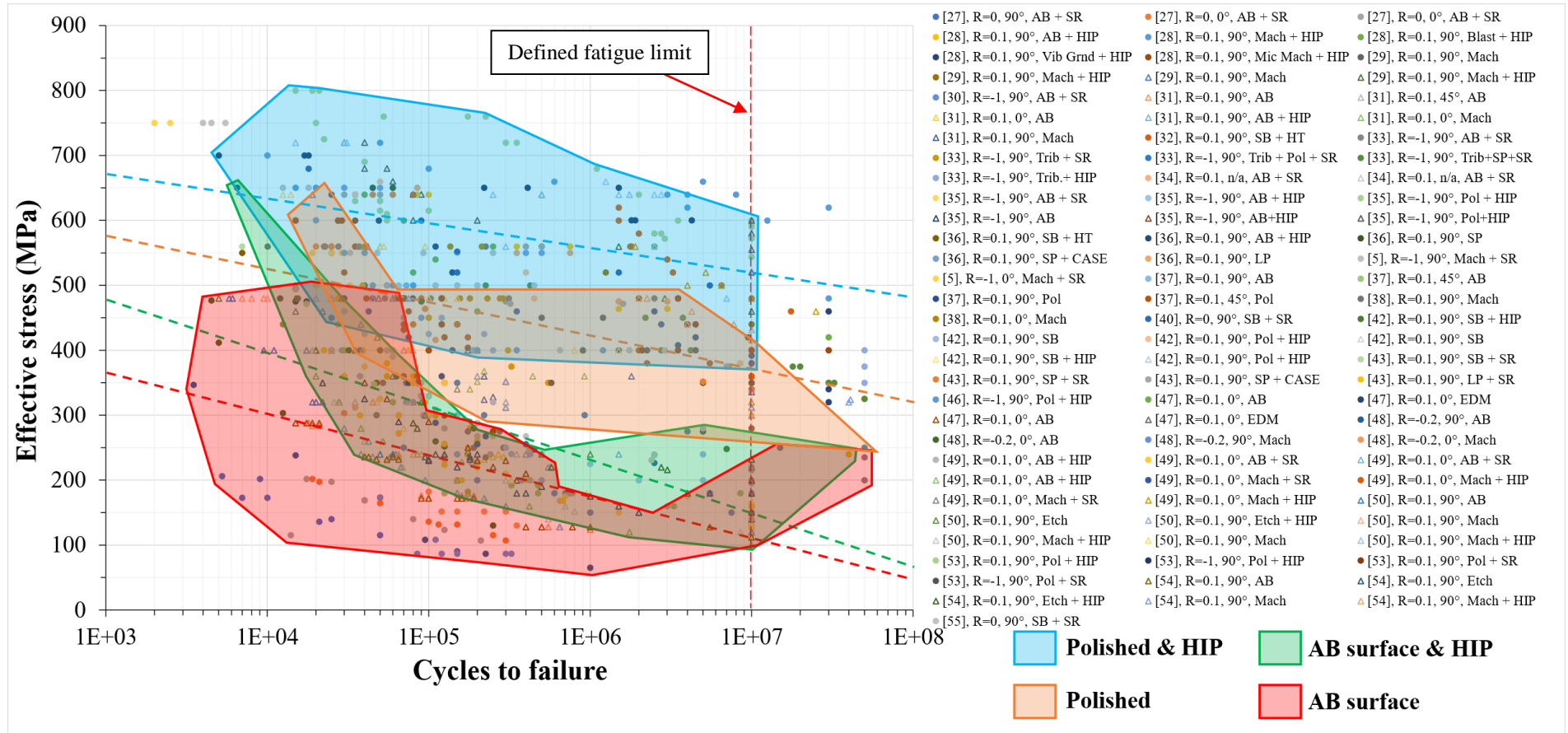


Figure 3: S-N chart showing fatigue data from PBF specimens. LB-PBF specimens are denoted by a filled circle, EB-PBF specimens are denoted by a hollow triangle. Fatigue data from specimens with polished surfaces, with and without HIP, as well as fatigue data from specimens with as-built surfaces, with and without HIP, are signified using coloured polygons. Effective stress is calculated according to the Walker method (equation 4). [27-31, 33-37, 42, 43, 46-50, 53, 54, 56].

Table 6: Fatigue test conditions of laser-based (LB) and electron-beam (EB) PBF Ti-6Al-4V with surface identified as: as-built (AB), sandblasted (SB), machined (M), tribofinished (TB), polished (P), electro-discharge machining (EDM), shot peened (SP), laser peened (LP), etched (E), vibratory ground surface (VG). Heat treatment defined as stress relieve (SR), Hot Isostatic Pressing (HIP), CASE (C), stress ratio (R), Fatigue test method, include rotating beam bending (RBB), four-point bending (4PB) and three-point bending (3PB). Data not reported (-).

Ref.	PBF method	Surface	HT	R	Fatigue test method	Frequency (Hz)	Runout limit (cycles)
[28]	LB	AB, SB, M, VG	SR, HIP	0.1	Axial	110	3E7
[12]	LB, EB	AB, TB	AB, SR, HIP	-1	RBB	85-96	1E7
[29]	LB, EB	M	AB, HIP	0.1	Axial	30	1E7
[31]	EB	AB	AB	0.1	Axial	10	1E7
[32]	LB	SB	SR	0.1	Axial	50	1E7
[33]	LB	AB, TB, P, SP	SR, HIP	-1	Axial	150	5E7
[34]	LB, EB	AB	SR	0.1	Axial	150	1E7
[5]	LB	M	SR	-1	Axial	20	1E7
[43]	LB	SB, SP, LP	SR, C	0.1	4PB	8	5E6
[46]	LB, EB	M, P	SR, HIP	-1	Axial	10, 19E3	2E6, 3E9
[50]	EB	AB, E, M	AB, HIP	0.1	Axial	10	1E6
[54]	LB	AB, E, M	AB, HIP	0.1	Axial	10	1E6
[27]	LB	AB	SR	0	Plane bending	20	2E6
[30]	LB	AB	SR	0	Plane bending	15	2E6
[48]	LB	AB, M	AB	-0.2	Axial	20	1E6
[57]	LB	AB	HIP	-1	Axial	82	1E7
[58]	LB	P	AB	0.2	Axial	10	-
[56]	LB	AB, SP, P	SR, HIP	0.1	Axial	150	5E7
[59]	LB	AB, M, P	AB	-1	RBB	20-25	1E7
[42]	LB, EB	SB, Pol	HIP	0.1	Axial	20	5E6
[49]	LB, EB	AB, M	SR, HIP	0.1	Axial	n/a	1E7
[53]	LB	P	HIP	0.1, -1	Axial	50, 2E4	1E7
[35]	LB, EB	AB, P,	AB, SR, HIP	-1	RBB	60	1E7
[36]	LB	AB, SB, SP, LP	AB, SR, HIP, C	0.1	4PB	8	5E6
[37]	LB	AB	AB	0.1	Axial	50	1E7
[47]	LB, EB	AB, EDM	AB	0.1	3PB	10	-
[26]	LB	AB, M	SR	-1	Axial strain	Variable	2E7
[41]	LB	M	AB, SR	-1	Axial strain	Variable	4E6
[38]	LB	M	AB	0.1	Axial	10	-
[55]	LB	SB	SR	0	Axial	10	1E6
[40]	LB	SB	SR	0	Axial	10	1E6
[39]	LB	AB, SB	SR, HIP	-1	Axial	120	-

Table 7: Properties of laser-based (LB) and electron-beam (EB) PBF Ti-6Al-4V with as-built (AB) surfaces assessed in this research. AM method, surface processing and heat treatment (HT) identified as: sandblasted (SB) and hot isostatic pressing (HIP), build direction (BD), arithmetic mean surface roughness (R_a), stress ratio (R), effective fatigue stress in MPa (based on logarithmic fitting) at specific number of cycles, ultimate tensile strength (UTS), elongation at failure ($\Delta\%$). Data not reported (-).

PBF method	Surface & HT	BD	R_a (μm)	R	σ @1E4 cycles	σ @1E5 cycles	σ @1E6 cycles	UTS (MPa)	$\Delta\%$	Ref.
LB	HT*	-	-	-	-	-	-	895*	10*	[60]
LB	AB	0°	13.0	0.1	357	272	187	1096	12	[49]
			32	-0.2	358	167	0	1035	3.3	[48]
		45°	-	0.1	336	267	199	-	-	[37]
		90°	38.5	-0.2	266	146	27	-	-	[48]
			-	0.1	279	208	137	-	-	[54]
			12.0	0.1	381	294	207	-	-	[37]
	AB+HT	0°	13	0.1	359	274	188	1096	15	[34]
		90°	-	0	175	96	16	1325	4.5	[27]
			6.83	0.1	240	170	150	1090	10	[33]
			13.4	0	258	219	180	1176	12.9	[30]
			6.83	-1	324	294	264	1090	10	[33]
			12^	-1	441	322	204	1176	14	[35]
			11.7	0.1	506	327	149	-	-	[36]
			11.7	0.1	514	324	133	-	-	[43]
	AB+HIP	0°	13.0	0.1	402	301	201	949	13	[49]
		90°	15	0.1	354	304	254	-	-	[42]
			-	-1	404	330	257	980	22	[35]
			17.9	0.1	415	353	291	-	-	[28]
EB	AB	0°	27.1	0.1	276	216	156	965	6	[49]
		90°	44	0.1	285	205	126	-	-	[31]
			32^	-1	363	274	186	1046	20	[35]
			31.2	0.1	409	164	0	-	-	[50]
	AB+HT	0°	27.1	0.1	277	210	143	965	5	[34]
	AB+HIP	0°	27.1	0.1	336	243	150	833	14	[49]
		90°	35	0.1	317	264	211	-	-	[42]
			-	-1	355	287	219	986	22	[35]

*These values represent the minimum requirements for HT Ti-6Al-4V manufactured by LB-PBF as stated by *ASTM F2924-14* [60]

^Areal roughness presented, not profile i.e. S_a used instead of R_a .

Table 8: Properties of laser-based (LB) and electron-beam (EB) PBF Ti-6Al-4V after surface processing assessed in this research. Surface processing and heat treatment (HT) identified as: as-built surface (AB), tribofinished (TB), machined (M), etched (E), vibratory ground surface (VG), corundum blasted (CB), laser peened (LP), shot peened (SP) and polished (Pol), build direction (BD), arithmetic mean surface roughness (R_a), stress ratio (R), effective fatigue stress in MPa (based on logarithmic fitting) at specific number of cycles, ultimate tensile strength (UTS), elongation at failure ($\Delta\%$). Data not reported (-).

PBF method	Surface & HT	BD	R_a (μm)	R	σ @1E4 cycles	σ @1E5 cycles	σ @1E6 cycles	UTS (MPa)	$\Delta\%$	Ref.
LB	SP	90°	3.36	-1	611	537	462	-	-	[59]
			4.6	0.1	660	546	432	-	-	[36]
	SP+CASE	90°	2.7	0.1	692	593	494	-	-	[43]
			2.7	0.1	705	597	488	-	-	[36]
	SP+SR	90°	4.6	0.1	635	532	430	-	-	[43]
	LP+SR	90°	10.2	0.1	757	636	514	-	-	[43]
	CB + HIP	90°	10.1	0.1	552	520	488	-	-	[28]
	VG+HIP	90°	0.9	0.1	539	489	438	-	-	[28]
	TB+HIP	90°	4.96	-1	478	447	417	960	14	[33]
	M	0°	7.67	0.1	480 @ 79,889 cycles			925	6.5	[47]
			0.89	-0.2	408	229	51	-	-	[48]
		90°	0.89	-0.2	190	112	34	-	-	[48]
			-	0.1	449	389	328	1300	6.5	[29]
	M+HT	0°	-	0.1	623	551	478	-	-	[49]
		90°	-	-1	650	550	425	953	16	[5]
	M+HIP	0°	-	0.1	753	668	583	-	-	[49]
		90°	0.4	0.1	514	476	437	-	-	[28]
			-	0.1	659	581	503	-	-	[54]
			-	0.1	705	617	528	925	16	[29]
			0.3	0.1	754	704	654	-	-	[28]
	E+HIP	90°	-	0.1	302	271	240	-	-	[54]
	Pol	90°	0.54	-1	472	473	474	-	-	[33]
	Pol+HIP	90°	-	-1	630	484	338	-	-	[46]
			-	-1	673	644	615	-	-	[35]
			-	-1	702	665	627	-	-	[53]
			-	0.1	712	593	475	-	-	[42]
			-	0.1	842	747	652	-	-	[53]
EB	E	90°	8.92	0.1	469	345	222	-	-	[50]
	M	0°	5.12	0.1	480 @ 48,926 cycles			775	2.5	[47]
		90°	0.13	0.1	463	218	0	-	-	[50]
			-	0.1	617	506	395	1050	14	[29]
			0.05	0.1	645	520	394	-	-	[50]
	M+HT	0°	-	0.1	478	381	284	-	-	[49]
	E+HIP	90°	8.92	0.1	515	365	215	-	-	[50]
	M+HIP	0°	-	0.1	741	656	571	-	-	[49]
		90°	0.13	0.1	469	305	142	-	-	[50]
			0.05	0.1	745	671	598	-	-	[50]
			-	0.1	870	726	583	1000	19	[29]
	Pol+HIP	90°	-	-1	701	654	606	-	-	[35]
			-	0.1	788	727	665	-	-	[42]

*Roughness characterised before HIP but assumed to be the same after HIP.

^Areal roughness presented, not profile i.e. S_a used instead of R_a .

Table 9: Properties of laser-based (LB) and electron-beam (EB) PBF Ti-6Al-4V after Hot Isostatic Pressing (HIP) assessed in this research. Surface processing and heat treatment (HT) identified as: as-built surface (AB), tribofinished (TB), machined (M), etched (E), vibratory ground surface (VG) and polished (Pol), build direction (BD), arithmetic mean surface roughness (R_a), stress ratio (R), effective fatigue stress in MPa (based on logarithmic fitting) at specific number of cycles, ultimate tensile strength (UTS), elongation at failure ($\Delta\%$). Data not reported (-).

PBF method	Surface & HT	BD	R_a (μm)	R	σ @1E4 cycles	σ @1E5 cycles	σ @1E6 cycles	UTS (MPa)	$\Delta\%$	Ref.
LB	AB + HIP	90°	17.9	0.1	415	353	291	-	-	[28]
			9.8	0.1	516	406	296	-	-	[36]
			10.1	0.1	552	520	488	-	-	[28]
	TB + HIP	90°	4.96	-1	478	447	417	960	14	[33]
	E + HIP	90°	-	0.1	302	271	240	-	-	[54]
	VG + HIP	90°	0.9	0.1	539	489	438	-	-	[28]
	M + HIP	90°	0.4	0.1	514	476	437	-	-	[28]
			-	0.1	659	581	503	-	-	[54]
			-	0.1	705	617	528	925	16	[29]
			0.3	0.1	754	704	654	-	-	[28]
	Pol + HIP	90°	-	-1	630	484	338	-	-	[46]
			-	-1	673	644	615	-	-	[35]
			-	-1	701	654	606	-	-	[35]
			-	-1	702	665	627	-	-	[53]
			-	0.1	842	747	652	-	-	[53]
EB	AB + HIP	90°	12*^	-1	355	287	219	-	-	[35]
	Etch + HIP	90°	8.92*	0.1	515	365	215	-	-	[50]
	M + HIP	90°	0.13*	0.1	469	305	142	-	-	[50]
			0.05*	0.1	745	671	598	-	-	[50]
			-	0.1	870	726	583	1000	19	[29]

*Roughness characterised before HIP but assumed to be the same after HIP.

^Areal roughness presented, not profile i.e. S_a used instead of R_a .

4.2 Surface roughness comparison

The inherent surface roughness associated with PBF is well understood to compromise fatigue performance. Numerous studies have shown marked improvement in fatigue life after surface treatments that reduce as-manufactured AM surface roughness [28, 34, 36]. Fatigue data which is accompanied by arithmetic mean surface roughness (R_a) data was identified and subject to logarithmic regression; from this regression effective stresses at fatigue lives of 1E4, 1E5 and 1E6 cycles were identified (Table 7,8,9). This data is plotted (Figure 4) to characterise the impact of roughness on observed fatigue response, with the following key observations:

- For the fatigue data assessed, surface roughness is reported to varying degrees. For specimens with as-built surface conditions, surface roughness is reported for 78% of cases (Table 7). For test data obtained from either processed surface conditions or HIP, only 55% of data is accompanied by roughness data (Table 8 and 9).
- Of this reported surface roughness, the arithmetic mean = roughness, R_a is by far the most commonly reported roughness parameter, followed by maximum roughness height, R_z , while only one paper reported maximum valley depth, R_v [42].

- As expected from the underlying influence on stress concentration, the summary data shows a general trend of decreasing effective stress with increasing roughness for any given fatigue life (Figure 4).
- Linear regression analysis was applied to each set of data (Figure 4). For this regression, the coefficient of determination (R^2) was found to lie in the range of 0.45 to 0.54 indicating a generally linear trend but with much variability in the prediction of effective stress from surface roughness alone. The high epistemic and aleatory variability serves to remind of the importance of documenting relevant variables in the reporting of fatigue test data.

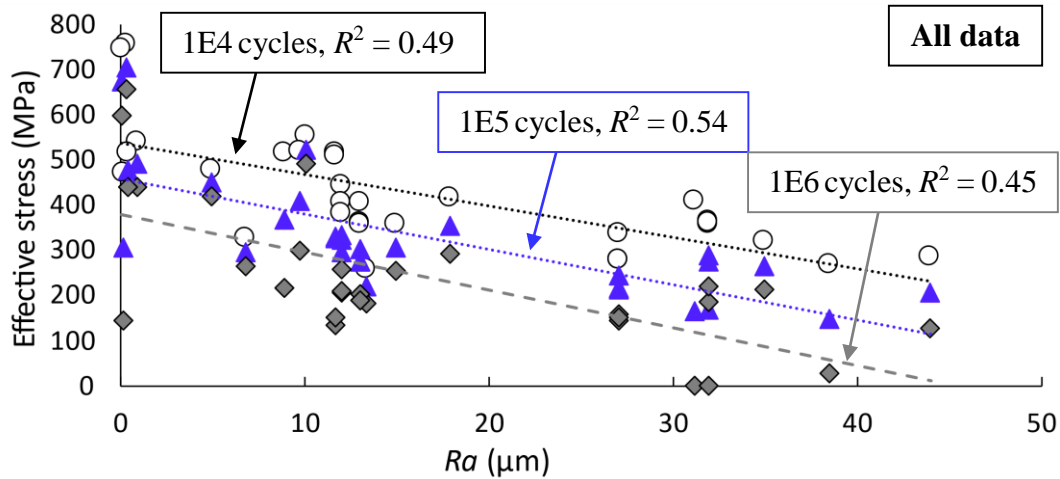


Figure 4: Arithmetic mean roughness, R_a , versus maximum stress for all AM fatigue data analysed in this research that released R_a values. Coefficient of determination (R^2) are listed for the regression line of each data series.

4.3 Microstructure and chemical composition comparison

The original patent for Ti-6Al-4V confirms the sensitivity of this alloy to variation in composition and phase. For a vanadium content between 3% and 5%, increasing aluminium content (up to 6%) increases tensile strength and ductility. Weldability properties are retained with vanadium content up to 4%, however increasing this up to 6% achieves maximum tensile strength with minimal adverse effect on ductility. To restrict embrittlement, oxygen and carbon should be $<0.1\%$, nitrogen $<0.07\%$ and hydrogen $<0.03\%$ [61]. *ASTM F2924-14 'Additive Manufacturing Titanium-6 Aluminum-4 Vanadium with Powder Bed Fusion'* stipulates minimum and maximum percentages of chemical elements in PBF components. These specifications are identical to the requirements for wrought alloys in *ASTM F1472-20* & *ISO 5832-3*. Note that for both *ASTM F2924-14* and *ASTM F1472-20* the allowable levels of minor elements i.e. nitrogen and oxygen are conservative when compared to the specified limits of the original Ti-6Al-4V patent. This is linked to high oxygen content resulting in poor ductility and crack growth resistance [62].

Of the AM Ti-6Al-4V fatigue data assessed in this research, applicability index for $\omega_{C,2}$, chemical composition data, was only 39% (Figure 1). Of the research that reported composition data, 46% was nominal data provided by powder manufacturers or *ASTM*

standards. Although the vast majority of reported composition data fell within the recommended range for Ti-6Al-4V, data outside of the standard allowable range was observed, for example [46].

The documentation criteria associated with microstructure and grain size description, ω_{C_5} , was reported by only 42% of the assessed fatigue data (Figure 1). Of this assessed data, microstructure was reported for 61% of the data and grain size measurements were reported by 21%. These below average results indicate that microstructural data is not being prioritised in the reporting of AM fatigue research, despite its significance to material fatigue response.

5 Discussion

AM reporting standard *ASTM F2971-21* focuses on the documentation of AM processes and materials to ensure repeatability in specimen reporting. This documentation includes: build layout and orientation; feedstock and powder recycling; post-processing and heat treatment; surface machining and other surface modification steps. Despite the extensive characterisation of material and processing required by AM reporting standard *ASTM F2971-21*, no mechanical properties are required to be reported according to the specified requirements, therefore, for fatigue applications additional reporting requirements are necessary. Fatigue reporting standard *ASTM E468-18* [24] was created to reduce uncertainty for fatigue data reported for traditional manufacturing methods. There is also a focus on identifying potential material anisotropy associated with mechanical working; an attribute that reveals the traditional manufacturing heritage of this standard, which are not directly relevant to the relevant opportunities and challenges inherent to AM. These two standards should be combined in order to accommodate the well-defined requirements of fatigue testing along with the unique AM characteristics.

By assessing the requirements of both AM and fatigue standards, as well as their correlation, a series of documentation criteria are identified that represent the core requirements of AM fatigue reporting, ω_{C_i} , (Table 5). In addition to existing fatigue relevant (Table 2) and identified AM relevant documentation requirements (Table 3), we propose that these documentation requirements provide a robust mechanism to characterise the quality of AM fatigue test documentation. This outcome can be used: to aid researchers in generating data that maximises the applicability of fatigue data by clearly documenting test procedures and manufacturing attributes; as a mechanism for design engineers to quantify (and thereby vet) the uncertainty associated with reported data within a specific area of interest; and, for fatigue researchers to identify scenarios with high levels of uncertainty and as such present a novel research opportunity.

The proposed method was demonstrated for a large sample ($N > 30$) of published data documenting fatigue testing of AM Ti-6Al-4V specimens with a variety of post processing conditions. Although the observations of this data cannot be construed to be representative of all published AM fatigue data, it does highlight the potential for compromised applicability of AM fatigue data, even within peer reviewed published research. For example, for the data assessed, the average applicability index for combined documentation criteria, $\bar{\alpha}_C$, is 72% ($\bar{\alpha}_F = 64\%$, $\bar{\alpha}_{AM} = 67\%$) and no data set was observed

to achieve 100% reporting quality. Of the observed reporting, several pertinent aspects of AM fatigue testing were consistently deficient. For example, powder recycling procedures were excluded from all but 4% of analysed papers (Figure 1). This is a significant omission given that the fatigue response of machined samples is improved when using recycled powder as opposed to virgin powder, and that recycled powder also demonstrates enhanced flowability and reduces the size of internal defects [26]. Excluding specimen preparation information such as this introduces ambiguity to test results that may preclude their application to high-value or safety-critical system design.

The large ($N > 30$) dataset of AM fatigue (especially for the critically important PBF of Ti-6Al-4V) provides a unique opportunity for insight into both typical test methods and the variability that process attributes can incur on observed fatigue strength. For example, this dataset shows a variability in effective stress in the order of 100 MPa to 800 MPa. This variation can, to a degree, be reduced by further classification of the data into relevant sub-classifications. As expected, the polished surface condition is associated with the higher strength subset of data, whereas the lower strength specimens are associated with as-built surfaces. Polished specimens are typically not relevant to production components due to the inherent processing cost and complexity, as well as the risk of in-service damage countering the benefit of polished surfaces and compromising the in-service safety factor. For these scenarios, the benefit of HIP in enhancing the fatigue strength of as-built surfaces is evident and may justify its commercial application. These observations are provided for general interest and insight, it is anticipated that the summary dataset will be useful to future researchers that intend to correlate fatigue response with specific processing and test attributes (Tables 6-9).

6 Conclusions

The use of additive manufacturing (AM) is becoming more prevalent in high-value commercial applications, including for fatigue-limited components. However, in order to confidently adopt reported AM fatigue test data for these safety-critical or high-value applications, robust supporting documentation is essential. The proposed applicability indices for AM fatigue test reporting represent a significant advancement in existing methods for quantifying the applicability of fatigue test data to the emerging field of AM. These indices can be used to evaluate the quality of published AM fatigue test data, aid designers in identifying data with high applicability, and identify areas of low applicability that may be targeted for further research. This research also highlighted deficiencies in documentation for a highly relevant AM alloy (Ti-6Al-4V), emphasizing the need for rigorous assessment of AM fatigue data, even when peer-reviewed. The large dataset of PBF Ti-6Al-4V used in this study provides valuable insight into the variability that can occur in AM fatigue response, specifically in relation to as-built, polished, and HIP specimens. This data serves as a valuable resource for future research on independent variables of interest.

7 Data availability

The processed data required to reproduce these findings are available to download from https://github.com/RMIT-DFAM/Fatigue_Applicability.

8 References

1. Sanaei, N. and A. Fatemi, *Defects in additive manufactured metals and their effect on fatigue performance: A state-of-the-art review*. Progress in Materials Science, 2021. **117**.
2. Tanaka, K. and Y. Akiniwa, *Fatigue crack propagation behaviour derived from S-N data in very high cycle regime*. Fatigue and Fracture of Engineering Materials and Structures, 2002. **25**(8-9): p. 775-784.
3. Walker, K., *The effect of stress ratio during crack propagation and fatigue for 2024-T3 and 7075-T6 aluminum*. 1970.
4. Stanzl-Tschegg, S.E. and H. Mayer, *Fatigue and fatigue crack growth of aluminium alloys at very high numbers of cycles*. International journal of fatigue, 2001. **23**(1): p. 231-237.
5. Sun, W., et al., *Effects of build direction on tensile and fatigue performance of selective laser melting Ti6Al4V titanium alloy*. International journal of fatigue, 2020. **130**: p. 105260.
6. Choi, Y.R., et al., *Influence of deposition strategy on the microstructure and fatigue properties of laser metal deposited Ti-6Al-4V powder on Ti-6Al-4V substrate*. International Journal of Fatigue, 2020. **130**.
7. Xu, W., et al., *Ti-6Al-4V Additively Manufactured by Selective Laser Melting with Superior Mechanical Properties*. JOM (1989), 2015. **67**(3): p. 668-673.
8. Molaei, R., et al., *Fatigue of additive manufactured Ti-6Al-4V, Part II: The relationship between microstructure, material cyclic properties, and component performance*. International journal of fatigue, 2020. **132**: p. 105363.
9. Qian, M., et al., *Additive manufacturing and postprocessing of Ti-6Al-4V for superior mechanical properties*. MRS Bulletin, 2016. **41**(10): p. 775-783.
10. Afroz, L., et al., *Fatigue behaviour of laser powder bed fusion (L-PBF) Ti-6Al-4V, Al-Si-Mg and stainless steels: a brief overview*. International Journal of Fracture, 2022. **235**(1): p. 3-46.
11. Hrabe, N., T. Gnäupel-Herold, and T. Quinn, *Fatigue properties of a titanium alloy (Ti-6Al-4V) fabricated via electron beam melting (EBM): Effects of internal defects and residual stress*. International Journal of Fatigue, 2017. **94**: p. 202-210.
12. Chastand, V., et al., *Comparative study of fatigue properties of Ti-6Al-4V specimens built by electron beam melting (EBM) and selective laser melting (SLM)*. Materials characterization, 2018. **143**: p. 76-81.
13. Emanuelli, L., et al., *Effect of heat treatment temperature and turning residual stresses on the plain and notch fatigue strength of Ti-6Al-4V additively manufactured via laser powder bed fusion*. International Journal of Fatigue, 2022. **162**.
14. Kumar, P. and U. Ramamurty, *Microstructural optimization through heat treatment for enhancing the fracture toughness and fatigue crack growth resistance of selective laser melted Ti6Al4V alloy*. Acta materialia, 2019. **169**: p. 45-59.
15. Molaei, R., A. Fatemi, and N. Phan, *Notched fatigue of additive manufactured metals under axial and multiaxial loadings, Part I: Effects of surface roughness and HIP and comparisons with their wrought alloys*. International Journal of Fatigue, 2021. **143**.
16. Pegues, J.W., et al., *Fatigue of additive manufactured Ti-6Al-4V, Part I: The effects of powder feedstock, manufacturing, and post-process conditions on the resulting microstructure and defects*. International journal of fatigue, 2020. **132**: p. 105358.
17. Murakami, Y., *Chapter 2 - Stress Concentration*, in *Metal Fatigue*, Y. Murakami, Editor. 2002, Elsevier Science Ltd: Oxford. p. 11-24.

18. Fox, J.C., S.P. Moylan, and B.M. Lane, *Effect of Process Parameters on the Surface Roughness of Overhanging Structures in Laser Powder Bed Fusion Additive Manufacturing*. Procedia CIRP, 2016. **45**: p. 131-134.
19. Masuo, H., et al., *Influence of defects, surface roughness and HIP on the fatigue strength of Ti-6Al-4V manufactured by additive manufacturing*. International Journal of Fatigue, 2018. **117**: p. 163-179.
20. du Plessis, A. and S. Beretta, *Killer notches: The effect of as-built surface roughness on fatigue failure in AlSi10Mg produced by laser powder bed fusion*. Additive manufacturing, 2020. **35**: p. 101424.
21. Strano, G., et al., *Surface roughness analysis, modelling and prediction in selective laser melting*. Journal of materials processing technology, 2013. **213**(4): p. 589-597.
22. Pegues, J., et al., *Surface roughness effects on the fatigue strength of additively manufactured Ti-6Al-4V*. International journal of fatigue, 2018. **116**: p. 543-552.
23. Leary, M. and C. Burvill, *Applicability of published data for fatigue- limited design*. Quality and reliability engineering international, 2009. **25**(8): p. 921-932.
24. E468-18, A., *Standard Practice for Presentation of Constant Amplitude Fatigue Test Results for Metallic Materials*. 2018, ASTM International: West Conshohocken, PA.
25. F2971-21, A., *Standard Practice for Reporting Data for Test Specimens Prepared by Additive Manufacturing*. 2021, ASTM International: West Conshohocken, PA.
26. Carrion, P.E., et al., *Powder Recycling Effects on the Tensile and Fatigue Behavior of Additively Manufactured Ti-6Al-4V Parts*. JOM (1989), 2018. **71**(3): p. 963-973.
27. Nicoletto, G., *Anisotropic high cycle fatigue behavior of Ti-6Al-4V obtained by powder bed laser fusion*. International journal of fatigue, 2017. **94**: p. 255-262.
28. Bagehorn, S., J. Wehr, and H.J. Maier, *Application of mechanical surface finishing processes for roughness reduction and fatigue improvement of additively manufactured Ti-6Al-4V parts*. International Journal of Fatigue, 2017. **102**: p. 135-142.
29. Zhao, X., et al., *Comparison of the microstructures and mechanical properties of Ti-6Al-4V fabricated by selective laser melting and electron beam melting*. Materials & design, 2016. **95**: p. 21-31.
30. Nicoletto, G., *Directional and notch effects on the fatigue behavior of as-built DMLS Ti6Al4V*. International journal of fatigue, 2018. **106**: p. 124-131.
31. Persenot, T., et al., *Effect of build orientation on the fatigue properties of as-built Electron Beam Melted Ti-6Al-4V alloy*. International Journal of Fatigue, 2019. **118**: p. 65-76.
32. Gong, H., et al. *Effect of defects on fatigue tests of as-built Ti-6Al-4V parts fabricated by selective laser melting*. in *Solid freeform fabrication symposium*. 2012. University of Texas Austin, Texas.
33. Benedetti, M., et al., *The effect of post-sintering treatments on the fatigue and biological behavior of Ti-6Al-4V ELI parts made by selective laser melting*. Journal of the mechanical behavior of biomedical materials, 2017. **71**: p. 295-306.
34. Greitemeier, D., et al., *Effect of surface roughness on fatigue performance of additive manufactured Ti-6Al-4V*. Materials Science and Technology (United Kingdom), 2016. **32**(7): p. 629-634.
35. Nakatani, M., et al., *Effect of Surface Roughness on Fatigue Strength of Ti-6Al-4V Alloy Manufactured by Additive Manufacturing*. Procedia Structural Integrity, 2019. **19**: p. 294-301.

36. Navarro, C., et al., *Effect of surface treatment on the fatigue strength of additive manufactured Ti6Al4V alloy*. Frattura ed Integrità Strutturale, 2020. **14**(53): p. 337-344.
37. Wycisk, E., et al., *Effects of Defects in Laser Additive Manufactured Ti-6Al-4V on Fatigue Properties*. Physics procedia, 2014. **56**: p. 371-378.
38. Walker, K.F., Q. Liu, and M. Brandt, *Evaluation of fatigue crack propagation behaviour in Ti-6Al-4V manufactured by selective laser melting*. International journal of fatigue, 2017. **104**: p. 302-308.
39. Dallago, M., et al., *Fatigue and biological properties of Ti-6Al-4V ELI cellular structures with variously arranged cubic cells made by selective laser melting*. J Mech Behav Biomed Mater, 2018. **78**: p. 381-394.
40. Razavi, S.M.J., P. Ferro, and F. Berto, *Fatigue assessment of Ti-6Al-4V circular notched specimens produced by selective laser melting*. Metals, 2017. **7**(8).
41. Sterling, A.J., et al., *Fatigue behavior and failure mechanisms of direct laser deposited Ti-6Al-4V*. Materials science & engineering. A, Structural materials : properties, microstructure and processing, 2016. **655**: p. 100-112.
42. Kahlin, M., H. Ansell, and J.J. Moverare, *Fatigue behaviour of notched additive manufactured Ti6Al4V with as-built surfaces*. International journal of fatigue, 2017. **101**: p. 51-60.
43. Aguado-Montero, S., et al., *Fatigue behaviour of PBF additive manufactured Ti6Al4V alloy after shot and laser peening*. International Journal of Fatigue, 2022. **154**: p. 106536.
44. Tarik Hasib, M., et al., *Fatigue crack growth behavior of laser powder bed fusion additive manufactured Ti-6Al-4V: Roles of post heat treatment and build orientation*. International journal of fatigue, 2021. **142**: p. 105955.
45. Kahlin, M., H. Ansell, and J. Moverare, *Fatigue crack growth for through and part-through cracks in additively manufactured Ti6Al4V*. International Journal of Fatigue, 2022. **155**: p. 106608.
46. Günther, J., et al., *Fatigue life of additively manufactured Ti-6Al-4V in the very high cycle fatigue regime*. International journal of fatigue, 2017. **94**: p. 236-245.
47. Chan, K.S., et al., *Fatigue Life of Titanium Alloys Fabricated by Additive Layer Manufacturing Techniques for Dental Implants*. Metallurgical and materials transactions. A, Physical metallurgy and materials science, 2012. **44**(2): p. 1010-1022.
48. Edwards, P. and M. Ramulu, *Fatigue performance evaluation of selective laser melted Ti-6Al-4V*. Materials science & engineering. A, Structural materials : properties, microstructure and processing, 2014. **598**: p. 327-337.
49. Greitemeier, D., et al., *Fatigue performance of additive manufactured TiAl6V4 using electron and laser beam melting*. International journal of fatigue, 2017. **94**: p. 211-217.
50. Sun, Y.Y., et al., *Fatigue Performance of Additively Manufactured Ti-6Al-4V: Surface Condition vs. Internal Defects*. JOM (1989), 2020. **72**(3): p. 1022-1030.
51. Leuders, S., et al., *On the mechanical behaviour of titanium alloy TiAl6V4 manufactured by selective laser melting: Fatigue resistance and crack growth performance*. International journal of fatigue, 2013. **48**: p. 300-307.
52. Fatemi, A., et al., *Torsional fatigue behavior of wrought and additive manufactured Ti-6Al-4V by powder bed fusion including surface finish effect*. International journal of fatigue, 2017. **99**: p. 187-201.
53. Wycisk, E., et al., *Fatigue Performance of Laser Additive Manufactured Ti-6Al-4V in Very High Cycle Fatigue Regime up to 10⁹ Cycles*. Frontiers in materials, 2015. **2**.

54. Persenot, T., et al., *Fatigue performances of chemically etched thin struts built by selective electron beam melting: Experiments and predictions*. Materialia, 2020. **9**: p. 100589.
55. Razavi, S.M.J., et al., *Fatigue strength of blunt V-notched specimens produced by selective laser melting of Ti-6Al-4V*. Theoretical and Applied Fracture Mechanics, 2018. **97**: p. 376-384.
56. Benedetti, M., et al., *Low- and high-cycle fatigue resistance of Ti-6Al-4V ELI additively manufactured via selective laser melting: Mean stress and defect sensitivity*. International journal of fatigue, 2018. **107**: p. 96-109.
57. Kasperovich, G. and J. Hausmann, *Improvement of fatigue resistance and ductility of TiAl6V4 processed by selective laser melting*. Journal of Materials Processing Technology, 2015. **220**: p. 202-214.
58. Qian, G., et al., *In-situ investigation on fatigue behaviors of Ti-6Al-4V manufactured by selective laser melting*. International journal of fatigue, 2020. **133**: p. 105424.
59. Mower, T.M. and M.J. Long, *Mechanical behavior of additive manufactured, powder-bed laser-fused materials*. Materials science & engineering. A, Structural materials : properties, microstructure and processing, 2016. **651**: p. 198-213.
60. F2924-14, A., *Standard specification for additive manufacturing titanium-6 aluminium-4 vanadium with powder bed fusion*. 2014, ASTM International: West Conshohocken, PA.
61. Abkowitz, S., *Heat treated titanium-aluminium-vanadium alloy*, U.s.p. office, Editor. 1959.
62. Fang, Z.Z., et al., *Powder metallurgy of titanium—past, present, and future*. International Materials Reviews, 2018. **63**(7): p. 407-459.

Declaration of interests

☒The authors declare that they have no known competing financial interests or personal relationships that could have appeared to influence the work reported in this paper.

☐The authors declare the following financial interests/personal relationships which may be considered as potential competing interests: